Jacobsson, Lars; Kjell, Gunnar; Kiuru, Risto; Suikkanen, Johannes

Wave velocity measurements in three directions on axially loaded water-saturated granite and gneiss core specimens

Published in:
Rock Mechanics for Natural Resources and Infrastructure Development - full papers

Published: 03/09/2019

Document Version
Peer-reviewed accepted author manuscript, also known as Final accepted manuscript or Post-print

Please cite the original version:
Jacobsson, L., Kjell, G., Kiuru, R., & Suikkanen, J. (2019). Wave velocity measurements in three directions on axially loaded water-saturated granite and gneiss core specimens. In S. A. B. da Fontoura, R. J. Rocca, & J. F. Pavón Mendoza (Eds.), *Rock Mechanics for Natural Resources and Infrastructure Development - full papers: Proceedings of the 14th International Congress on Rock Mechanics and Rock Engineering (ISRM 2019), September 13-18, 2019, Foz do Iguassu, Brazil* (pp. 1638-1645). (Proceedings in Earth and geosciences series; Vol. 6). CRC Press.

Wave velocity measurements in three directions on axially loaded water-saturated granite and gneiss core specimens

L. Jacobsson & G. Kjell
RISE Research Institutes of Sweden, Borås, Sweden

R. Kiuru
Aalto University School of Engineering, Department of Civil Engineering, Espoo, Finland

J. Suikkanen
Posiva Oy, Eurajoki, Finland

ABSTRACT: The density, porosity and mechanical properties from uniaxial compression and Brazilian tests along with measurements of the P- and S-wave velocities in axial and two lateral directions at unloaded state and at increasing axial load were conducted on cylindrical cores of veined gneiss and granitic pegmatoid. The specimens were sampled close to a tunnel wall (0.1–1.7 m depth) with the aim to find if there is an increasing amount of microcracks due to the excavation in a zone near the surface. Evidence of microcracks was found via the mechanical tests and the wave velocity measurements, due to increased mechanical stiffness and increasing wave velocities at loading. Anisotropy in in the gneiss specimens and also in the granitic pegmatoid was detected and measured via strain and wave velocity measurements. No clear evidence was found of increased amount of microcracks closer to the tunnel wall.

1 INTRODUCTION

Knowledge of the extent and properties of excavation damaged zone (EDZ) around deposition tunnels in underground repositories for spent nuclear fuel is part of the long-term safety assessment. Several projects for characterizing and studying the properties of EDZ have been carried out by e.g. various nuclear waste management organizations such as Posiva Oy in Finland and SKB in Sweden (Mustonen et al., 2010). The conducted studies indicate that each underground repository site has its own unique characteristics in terms of geological history, in-situ stress state and lithology along with the applied excavation methods, which make the development of EDZ to a large extent site specific.

This study, financed by Posiva Oy, belongs to the on-going investigations into characterization of excavation damage at the ONKALO research facility in Olkiluoto, Finland. The excavation damage was studied below the floor level of a specifically excavated ONK-TKU3620 niche located at the depth of -345 m. The major rock types prevailing in Posiva's EDZ study volume were foliated veined gneiss (VGN) and granitic pegmatoid (PGR).

It is known that the presence of microcracks in rock materials affects the propagation of elastic waves by lowering the wave propagation velocities as well as the stiffness and strength, and by increasing the apparent porosity. These properties including density were measured on rock core specimens extracted from the tunnel floor as a function of specimen depth, in order to determine whether EDZ effects could be measured from intact rock specimens obtained close to the excavated tunnel surface.

2 SPECIMENS

The specimens belonged to three different sets extracted from nominally 68 – 69 mm diameter cores with sampling depth from the tunnel surface in the range of 0.1 – 1.7 m. Specimens from Set 1a were only subjected to petrophysical testing of density (ρ), porosity (ϕ) and P- and S-wave velocities (v_p and v_s). P- and S-wave velocities were measured in the axial direction on the Set 2a specimens, and in the axial and two lateral directions on the Set 2b specimens at six different axial stress levels, 0, 2.5, 5, 10, 15 and 20 MPa. Finally, Set 2a specimens were subjected to Brazilian tests (BR) and Set 2b specimens to uniaxial compression tests (UCS). All measurements were conducted on specimens fully saturated in saline formation water from ONKALO. The number of specimens and tests are shown in Table 1. The VGN specimens had two different foliation directions in relation to the specimen axis.

Table 1. Specimen set, rock type, nominal length and number of measurements for each test method.

Set	rock type	L_{nom} mm	ρ, ϕ	v_p, v_s ax,ul	v_p, v_s ax,lo	v_p, v_s lat,lo	BR	UCS
Set 1a	VGN	50	10	10	-	-	-	-
Set 1a	PGR	50	10	10	-	-	-	-
Set 2a	VGN	30	20	20	-	-	19(*)	-
Set 2a	PGR	30	6	6	-	-	6	-
Set 2b	VGN	170	20	-	20	20	-	20
Set 2b	PGR	170	6	-	6	6	-	6

ax,ul = axial direction on unloaded specimens
ax,lo = axial direction at 6 different axial loads (0, 2.5, 5, 10, 15, 20 MPa)
lat,lo = two lateral directions at 6 different axial loads (0, 2.5, 5, 10, 15, 20 MPa)
(*) One specimen had uneven cylindrical surface and was excluded from mechanical testing.

3 METHODOLOGY

3.1 *Preparation*

The specimens were first prepared by cutting to suitable length for Brazilian tests, BR, (Set 2a) and uniaxial compression tests, UCS, (Set 2b) and finally grinding the planar end surfaces. The specimen dimensions were measured and the compliance of geometrical tolerances was checked according to ASTM (2004b). Strain gauge rosettes (120 ohm, three directions) with 20 mm gauge length from Kyowa were installed onto the BR and UCS specimens using a cyanoacrylate adhesive (Kyowa CC-33a). One strain gauge per BR specimen was installed onto the center on one of the plane surfaces just before the BR test.

Four strain gauges were installed onto each of the UCS specimens with a 90-degree division at mid-height with a nitrile rubber coating (M-Coat B from Micro-Measurements). Figure 1 shows the placement and orientations of the strain gauges. The strain gauges were installed on the specimens after the density and porosity measurements at water saturated condition.

3.2 *Density and porosity measurements*

Density and porosity procedures and measurements mostly followed ISRM (1979b). A deviation was that the specimens were dried and the mass of the oven-dry specimens was determined before water saturation. Specimens in Set 1a were water saturated, dried and measured two times. The oven-drying was done according to ISRM (1979b) both times. The first water saturation was conducted according to ISRM (1979b). The second time it followed CEN (2006) with an additional storage time in water of four weeks. The dry mass was not determined again the second time. The specimens from Set 2a and Set 2b were only dried and saturated one time with saturation following CEN (2006) with an additional storage time in water of four weeks.

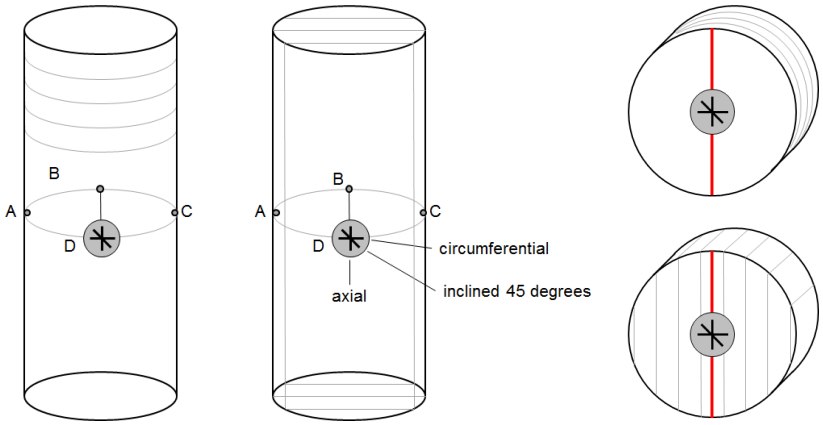

Figure 1. Placement and orientation of strain gauges on foliated specimens. Left: horizontal (0 degrees dip angle) foliation; Middle: vertical (90 degrees dip angle) foliation; Right: foliation directions Brazilian test specimens. Red line is the loading line.

3.3 *Waves in a transversely isotropic material*

The material properties in VGN can be approximated as transversely isotropic material and in PGR as isotropic material due the foliated and isotropic material structures. The wave velocities in a transversely isotropic material are

$$v_{p(||)} = v_{xx} = v_{yy} \tag{1}$$

$$v_{p(\perp)} = v_{zz} \tag{2}$$

$$v_{sh} = v_{xy} = v_{yx} \tag{3}$$

$$v_{sv} = v_{xz} = v_{yz} = v_{zx} = v_{zy} \tag{4}$$

where $v_{p(||)}$ is the P-wave propagating parallel to the isotropic plane and $v_{p(\perp)}$ is the P-wave propagating perpendicular to the isotropic plane. The velocity v_{sh} refers to the S-wave propagating and polarized parallel to the isotropic plane and v_{sv} refers to the S-wave propagating parallel and polarized perpendicular to the isotropic plane. For rock material, it is commonly observed that $v_{p(||)} > v_{p(\perp)}$ and $v_{sh} > v_{sv}$. The material orientations and wave velocities for a cylindrical geometry, representing the VGN specimens in the current investigations, are shown in Figure 2. For PGR the wave velocities are equal in all directions due to isotropy. See Jacobsson et al. (2019) for further details.

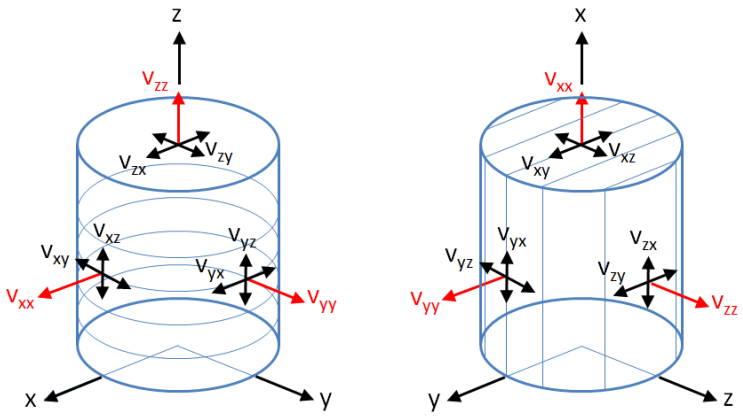

Figure 2. Wave velocities in a cylindrical specimen with transverse isotropic material. Left: isotropy plane perpendicular to the specimen axis; Right: isotropy plane parallel to the specimen axis.

3.4 *P- and S-wave velocity measurements*

A combined pulse generator and sampling device (ULT-100) and two types of piezoelectric sensors from GCTS, USA, were used. The first type was sensors for measuring wave velocities in the axial direction with piezoelectric crystals for both P- and S-waves were integrated inside 76 mm diameter steel loading platens that could sustain a load on a rock specimen up to compressive failure. The piezoelectric crystals for the S-wave measurement were arranged in a square pattern such that a rotational (torsional) shear wave is generated, and respectively measured. This sensor configuration implies that the propagating wave will partially be along the foliation plane and across the foliation plane when measurements are made in the axial direction on specimens with the foliation direction along with the specimen axis (cf. Figure 2) and the adherent wave velocity is denoted v_{shv}, where $v_{sh} < v_{shv} < v_{sv}$.

The second type was small sensors which had an aluminium housing that could be loaded up to 500 N to achieve a sufficient contact pressure for good wave transmission. The sensors contained only one piezoelectric crystal for either P- or S-wave. The piezoelectric crystals in the S-wave sensors were oriented such that a linear, one directional, shear wave was generated, and respectively measured. The piezoelectric crystals used in the sensors had a resonance frequency of 200 kHz. The setup is shown in Figure 3.

The measurements were carried out, as close as possible, on specimens at a water saturated condition. A coupling gel was used between the sensors and the specimen. Thin wave guides were in addition placed between the specimens and the sensors to accommodate for the specimen surface curvature at the measurements in the lateral direction

A standard measurement uncertainty was calculated according to the Guide to the Expression of Uncertainty in Measurement (JCGM, 2008) based on measurements on three aluminium reference specimens with different lengths, as devised by ASTM (2004a), and on the current measurements on rock specimens. The expanded uncertainty was calculated for the different types of measurements that were conducted and is based on a standard uncertainty multiplied by a coverage factor of k = 2, providing a level of confidence of approximately 95 %. A detailed description of the calculations is found in Jacobsson & Kjell (2017).

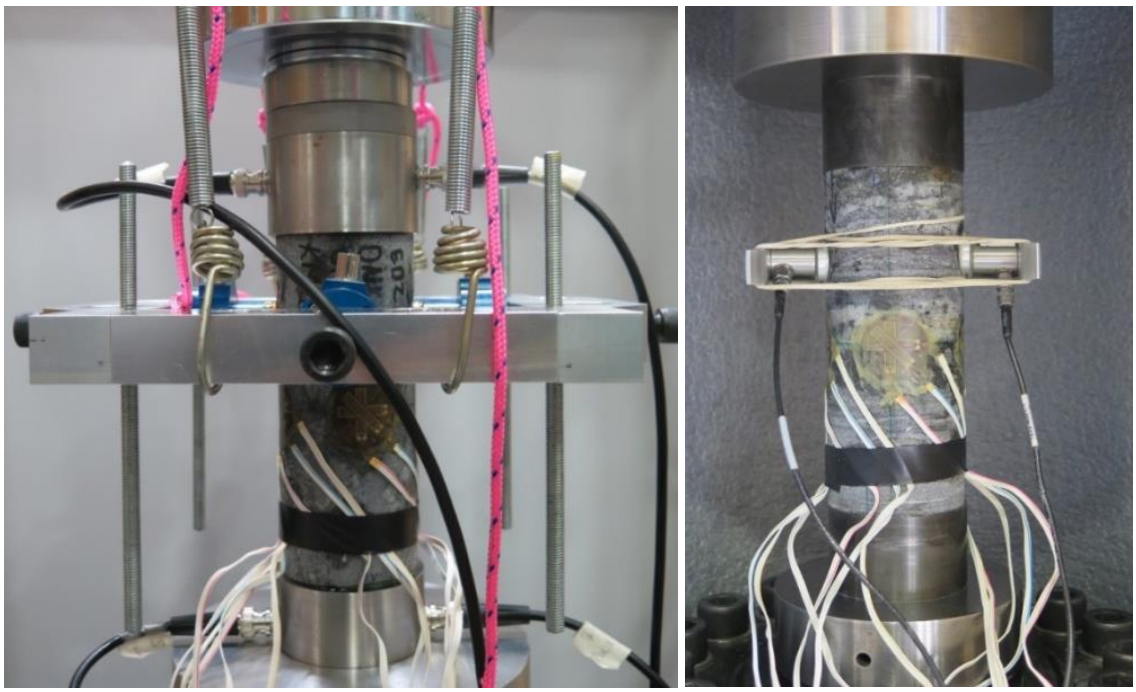

Figure 3. Left: Rock specimen placed between the loading platens with integrated piezoelectric crystals. The sensors for lateral measurements are mounted (blue), but not connected at this stage. The square frame is mounted slightly above the mid-height of the specimen. A small uplifting force to balance the gravity force from the mass of the rectangular frame and sensors is obtained by four hooks connected to springs. Right: Setup for the UCS tests with mounted AE-sensors.

3.5 *Brazilian and uniaxial compression tests*

Indirect tensile tests were carried out according to ISRM (1978a). Strain was measured in three directions. Four layers of paper masking tape were wrapped around on the cylindrical surface in order to obtain a padding thickness of 0.2 – 0.4 mm in accordance with ISRM (1978a).

The UCS tests were conducted with strain and acoustic emission (AE) measurements using a Micro-II Digital SE system from Physical Acoustic Corporation (PAC) for the AE measurements. Two acoustic emission sensors, R15a (PAC), were attached to the specimen via the same wave guides as at the wave velocity measurements in between. Vacuum/stopcock grease was used as coupling media. The UCS tests were carried out according to ISRM (1979a). The specimens were loaded up to failure at a rate of 0.5 MPa/s, except for the first two specimens which were loaded at 0.8 MPa/s. The loading rate was adjusted to come closer to a failure time of 5 minutes.

4 RESULTS

4.1 *Density and porosity on specimens from Set1a, Set2a and Set 2b*

Results from density and porosity measurements versus sampling depth for all three specimen sets are shown in Figure 4. Note that the specimen lengths are different in the different sets. Some of the higher porosity specimens from near the surface could be visually linked to excavation damage features (see Kiuru et al., 2019).

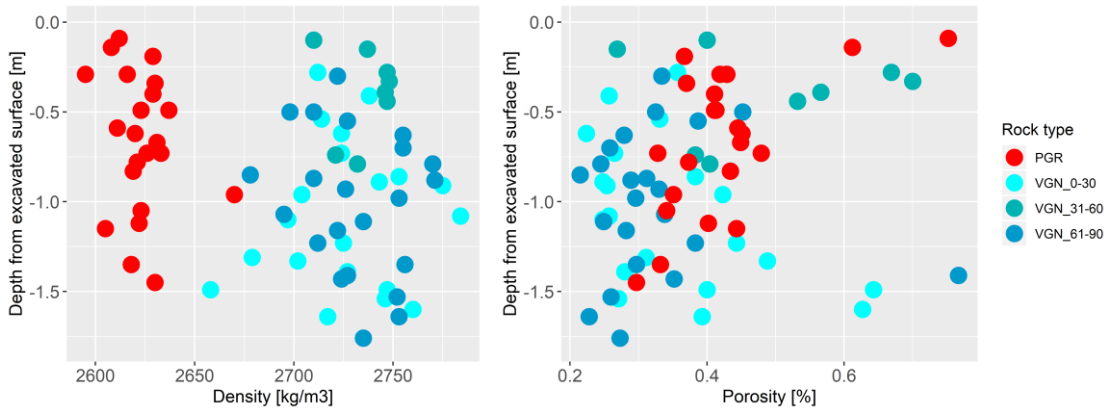

Figure 4. Left: Density as a function of sampling depth; Right: Porosity as a function of sampling depth. Rock type and foliation represented by colour.

4.2 *P- and S-wave velocity on specimens from Set1a, Set2a and Set 2b*

Results from the wave velocity measurements on unloaded specimens versus sampling depth from all three specimen sets are shown in Figure 5. Note that the specimen lengths are different in the different sets. The measurement of the wave velocities in the lateral direction were only made on the Set 2b specimens and there are thus fewer measurements of that type.

Wave velocities on three specimens subjected to an increasing axial load belonging to Set 2b are shown in Figure 6. The specimens represent the categories VGN 0, VGN 90 and PGR and were chosen to illustrate type cases related to the structural anisotropy. The results show good example of anticipated values of wave velocities in the axial and lateral directions as discussed in Section 3.3. It can be seen that the wave velocities in the axial direction increases with increasing axial load due to crack closure. Surprisingly, the wave velocities in the lateral directions also increased significantly during increasing axial loading. The ratio of the strains $\varepsilon_{circ,AC}/\varepsilon_{circ,BD}$ measured at 20 MPa axial stress (Figure 6) reflect anisotropy in the plane perpendicular to the specimen axis and complies with measured wave velocities. It was found that the strain ratio $\varepsilon_{circ,AC}/\varepsilon_{circ,BD}$ varied between c. 0.6 to 1.5 for the PGR specimens in spite of the

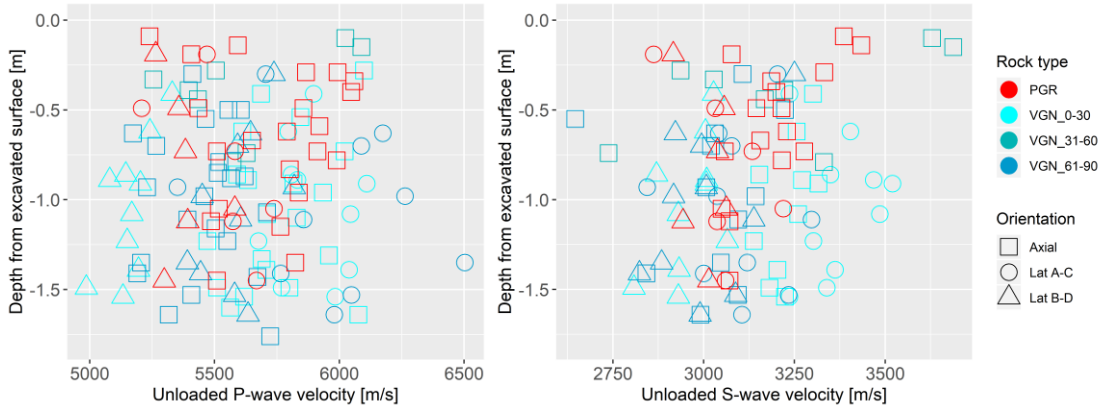

Figure 5. Wave velocities measured unloaded in the axial direction as a function of sampling depth. Left: P-wave velocity; Right: S-wave velocity. Rock type and foliation represented by colour, measurement orientation represented by shape (see Figure 1).

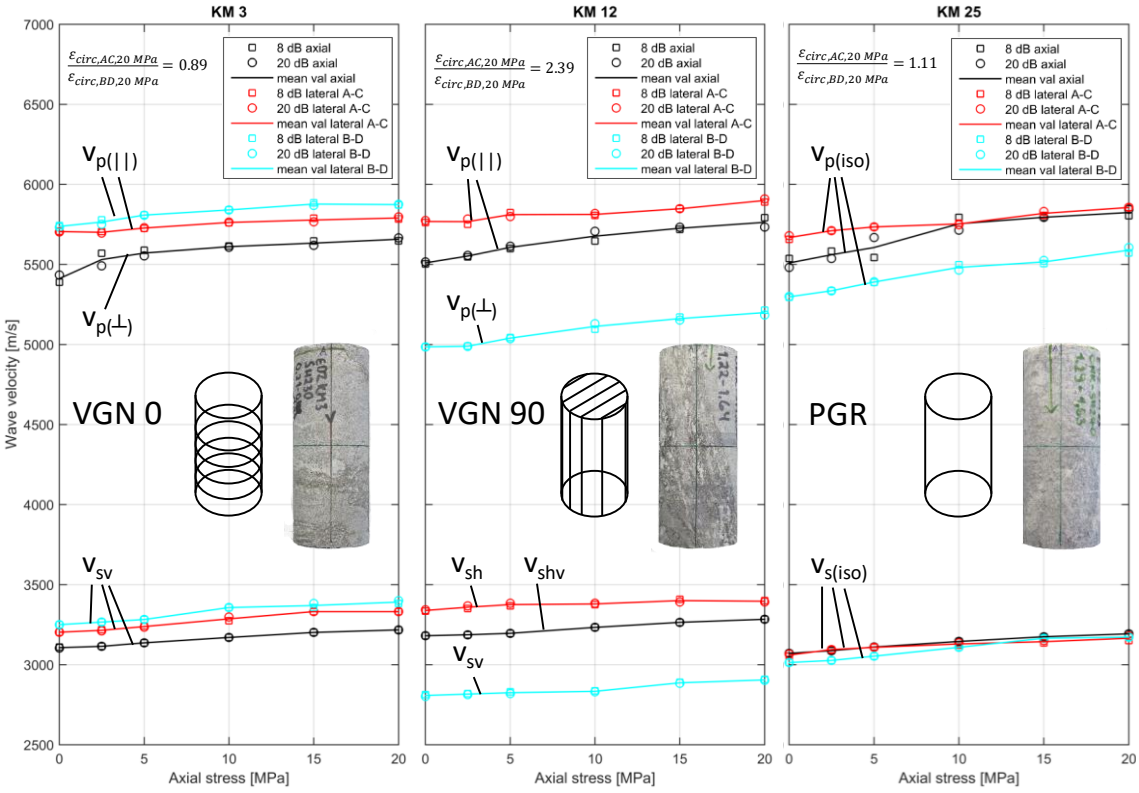

Figure 6. Wave velocities in three different directions at six load levels for specimen KM3, KM12 and KM25, specimen photos and foliation orientation.

isotropic microstructure (not shown here). A correlation to the ratio of the wave velocities was found. An explanation to this could be oriented microcracks within the specimens causing the measured anisotropy.

4.3 *Mechanical tests on specimens from Set 2a and Set 2b*

Results from the Brazilian tests on specimens from Set 2a are shown in Figure 7. Results from the uniaxial compression tests on specimens from Set 2b are shown in Figures 8 and 9. It shall be remarked that the elasticity parameters are based on an isotropic material response. The crack initiation stress and the uniaxial compressive strength are shown in Figure 9.

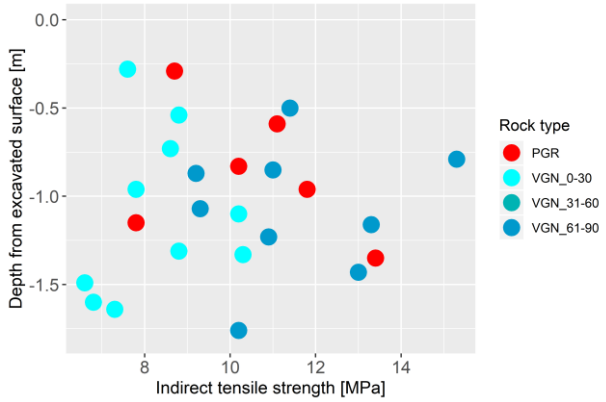

Figure 7. Indirect tensile strength in respect to depth.

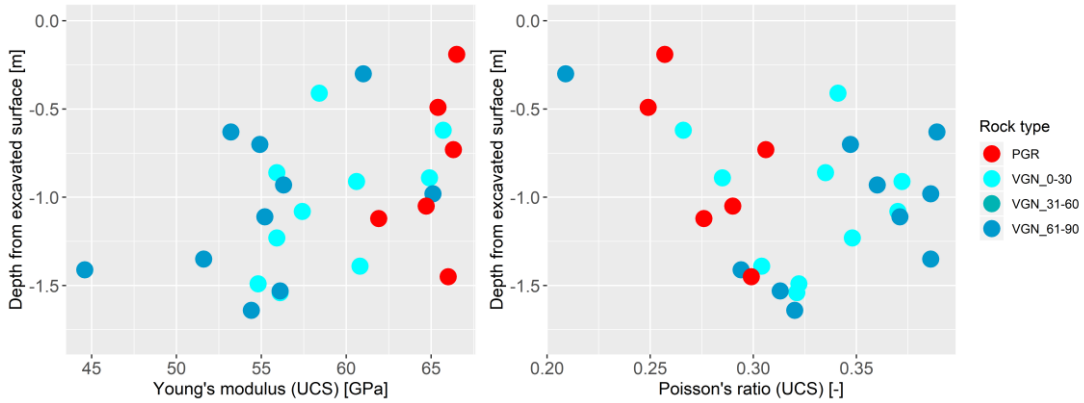

Figure 8. Left: Young's modulus in respect to depth; Right: Poisson's ratio in respect to depth.

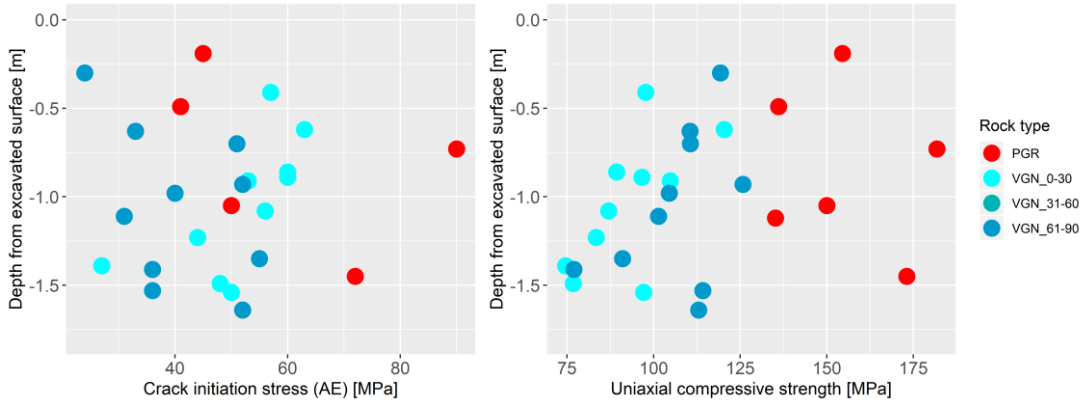

Figure 9. Left: Crack initiation stress and; Right: Uniaxial compressive strength in respect to depth.

5 DISCUSSION AND CONCLUSIONS

First obvious source of bias in the measurements is the specimen selection: as the specimens subjected to mechanical testing need to stay in one piece until the test, the most damaged sections simply cannot be sampled. Second, the effect of preparation on the specimens is unknown as there are no unprepared specimens for e.g. thin sections. This was however assumed to have a similar effect on all specimens due to the same procedure followed in preparation. The saturation procedure was changed from the one in ISRM (1979b) to the one in CEN (2006). First arrival picking poses challenges due to noisy onset of specifically the S-waves, and varying speci-

men sizes (both diameter and length), especially in respect to varying grain size, may have an effect on the picking accuracy. Finally, determination of mechanical properties is dependent on the assumption of linear elasticity. Various aspects that could affect the reliability of the measurements are described in more detail in the reports by Jacobsson et al. (2019) and Kiuru et al. (2019).

P- and S-wave velocity measurements were carried out at unloaded condition in one direction and at uniaxial compression in three orthogonal directions and at six different load levels. The increasing axial compression successively closed existing microcracks which showed up as increasing wave velocities. Microcracks oriented perpendicular to the core axis will theoretically be closed most efficiently and cracks with orientations deviating from this will be closed to a varying degree, while cracks parallel to the core axis should open. However, the wave velocities in all three directions increased. Varying levels of anisotropy were observed for most specimens, including PGR specimens. This means that assumptions of isotropy or transversal isotropy are not accurate for these specimens. Clear dependency on loading could be observed for both velocities, an increase of 5.9 % and 4.2 % in P- and S-wave velocities, respectively, were observed when loading was increased from approximately 0 MPa to 20 MPa. All other elastic parameters also showed a clear increase with increasing load, except for Poisson's ratio that is less sensitive to deformation. The results showed no clear sign of systematic anomalies close to the excavated surface in any of the measurements. This suggests that EDZ cannot be observed from the amount of microcracks based on these measurements. Further description of tests and results can be found in Jacobsson et al. (2019) and Kiuru et al. (2019).

DISCLAIMER AND ACKNOWLEDGEMENTS

The views expressed are those of the authors and do not necessarily reflect those of Posiva. We would like to thank Academy of Finland for funding (grants 297770 and 319798) and Posiva Oy for providing the possibility to publish the data.

REFERENCES

ASTM, 2004a. D 2845-00 (reapproved 2004). Standard test method for laboratory determination of pulse velocities and ultrasonic elastic constants of rock. ASTM International, West Conshohocken, USA.

ASTM, 2004b. D4543-04 Standard practices for preparing rock core specimens and determining dimensional and shape tolerances. ASTM International, West Conshohocken, USA.

CEN, 2006. EN 1936:2006 Natural stone test method - Determination of real density and apparent density, and of total and open porosity. CEN European Committee for Standardization.

ISRM, 1978a. Suggested methods for determining tensile strength of rock materials. Int J Rocks Mech Min Sci Geomech Abstr 15, pp. 99–103.

ISRM, 1978b. Suggested methods for determining sound velocity. Int J Rocks Mech Min Sci Geomech Abstr 15, pp. 53–58.

ISRM, 1979a. Suggested methods for determining the uniaxial compressive strength and deformability of rock materials. Int J Rocks Mech Min Sci Geomech Abstr 16, pp. 137–140.

ISRM, 1979b. Suggested methods for determining water content, porosity, density, absorption and related properties and swelling and slake-durability index properties. Int J Rocks Mech Min Sci Geomech Abstr 16, pp. 141–156.

Jacobsson, L. & Kjell, G., 2017. Measurement of p- and s-wave velocity in material using ultrasonics, RISE Report 2017:48, RISE Research Institutes of Sweden, 145 p.

Jacobsson, L., Kjell, G., Brander, L., Kiuru, R. 2019. EDZ Study Area in ONK-TKU-3620: Determination of Seismic Wave Velocities at Six Load Levels, Petrophysical and Rock Mechanical Properties of Drill Core Specimens. Posiva Oy, WR 2016-57. In press

JCGM, 2008. Evaluation of measurement data – Guide to the expression of uncertainty in measurement, JCGM 100:2008. Joint Committee for guides in metrology, JCGM.

Kiuru, R., Heikkinen, E., Kovács, D. and Jacobsson, L., 2019. EDZ Study Area in ONK-TKU-3620: Petrophysical, rock mechanics and petrographic testing and analysis conducted in drill core specimens between 2014 and 2016. Posiva Oy, Working Report 2017-56. In press.

Mustonen, S., Norokallio, J., Mellanen, S., Lehtimäki, T. and Heikkinen, E., 2010. EDZ09 Project and Related EDZ Studies in ONKALO 2008-2010. Posiva Oy, WR 2010-27.